

# Relaxed Conditional Statistical Shape Models and Their Application to Non-contrast Liver Segmentation

Sho Tomoshige<sup>1</sup>, Elco Oost<sup>1</sup>, Akinobu Shimizu<sup>1</sup>, Hidefumi Watanabe<sup>1</sup>,  
Hidefumi Kobatake<sup>1</sup>, and Shigeru Nawano<sup>2</sup>

<sup>1</sup> Graduate School of Bio-Applications and Systems Engineering,  
Tokyo University of Agriculture and Technology,  
Nakacho 2-24-16, Koganei-shi, Tokyo 184-8588, Japan  
{c\_r\_oost, simiz}@cc.tuat.ac.jp

<sup>2</sup> Department of Radiology, International University of Health and Welfare,  
Mita Hospital, 1-4-3 Mita, Minato-ku, Tokyo 108-8329, Japan

**Abstract.** This paper proposes a novel conditional statistical shape model (SSM) that allows a relaxed conditional term. The method is based on the selection formula and allows a seamless transition between the non-conditional SSM and the conventional conditional SSM. Unlike a conventional conditional SSM, the relaxed conditional SSM can take the reliability of the condition into account. Organ shapes estimated by the proposed SSM were used as shape priors for Graph Cut based segmentation. Results for liver shape estimation and subsequent liver segmentation show the benefit of the proposed model over conventional conditional SSMs.

**Keywords:** Conditional shape modeling, relaxation, liver segmentation.

## 1 Introduction

Graph Cut based segmentation [1] with a shape prior as regulating term in the optimization of the energy function has proven a valuable tool in medical image processing [2,3]. Using a set of image features that are extracted from the target image as the conditional term for a conditional SSM, for example as described in [4], a shape prior is estimated that will serve as a restricting term in the optimization of the energy function in Graph Cut segmentation. Given an appropriate shape prior the Graph Cut segmentation will improve. This benefit is the method's vulnerability as well: A poor quality shape prior will deteriorate the Graph Cut segmentation accuracy.

Relaxation of the condition, instead of applying the condition as a hard constraint, is essential in generating a shape prior. A relaxed conditional SSM should be able to bridge seamlessly between a non-conditional SSM and a conventional conditional SSM with hard constraints. Obtaining a method that allows such a seamless transition is the main aim of this paper, which is achieved by using the selection formula [5] for the calculation of the conditional covariance matrix and the conditional average.

Several conditional SSMs have been proposed. Baka et. al [6] propose a conditional SSM in which uncertainties of the conditions can be integrated. The algorithm

calculates a conditional covariance matrix, but does not calculate a conditional average. For a seamless transition between non-conditional SSM and conventional conditional SSM however, both the conditional covariance matrix and the conditional average are required. Syrkina et. al [7] propose a shape estimation method, that calculates a conditional distribution through a joint multivariate distribution of two statistical shape models; one representing the predictors and one for the shape that needs to be predicted. To minimize the prediction error, the number of shape modes retained for the two models is limited. In some cases this can lead to a considerable part of the training data that will be excluded from the model. Furthermore the algorithm requires an estimate of the noise variance, which is difficult to obtain.

The algorithm by de Bruijne et. al [4] uses the conventional conditional SSM with hard constraints, and extends it with ridge regression [8] to regularize the covariance matrix. Additionally, the introduction of ridge regression is an alternative approach to relax the conditional term of the SSM, because it allows the calculation of both the conditional covariance matrix and the conditional average. A ridge parameter of zero will result in the conventional conditional SSM with hard constraints, whereas a very large ridge parameter leads to the generic, non-conditional SSM. Hence, the range of the regulating term is between zero and infinity. The method proposed in this paper presents a more elegant transition, with a regulating term between zero and one. In addition, the identity matrix in ridge regression might not be suitable to relax the condition, because it enhances the influence of the weaker shape variations.

The benefit of the proposed method will be assessed by liver shape estimation, followed by liver segmentation in non-contrast CT images. Many state of the art algorithms for liver shape estimation and liver segmentation provide similar performance in relatively easy to segment images. The difficult to segment images, e.g. when the liver shape differs strongly from the average liver shape, remain challenging. Estimation of such shapes, based on image features, is difficult and can result in errors in the condition estimation. The subsequent segmentation is hampered by suboptimal shape estimation. This paper seeks the room for improvement for such cases. Presented results focus on difficult to segment images. Furthermore, because shape estimation by a ridge regression based conditional SSM is the closest related method, results of the proposed method will be compared with results obtained through ridge regression.

## 2 Conventional Conditional Statistical Shape Models

To train a level-set based SSM, a data set of  $N$  manually annotated images is used to create a signed distance map, in which voxel values represent the distance to the organ contour. Negative distances denote the organ's interior, positive distances signify the organ's exterior. The distance data is extracted to a one-dimensional column vector, sized  $M$ , and Principal Component Analysis is applied to create a SSM. Projection of the training samples onto the model results in the principal component score matrix  $b$ , as depicted in Fig. 1. Details on level set based SSM training can be found in [9].

To obtain conditional data, a number of features is calculated from the true label data for all training data samples. These features are combined in matrix  $X$ , which has  $N$  columns (number of training samples) and  $F$  rows (number of calculated features). Subsequently, an unseen test image is roughly segmented using maximum a posteriori

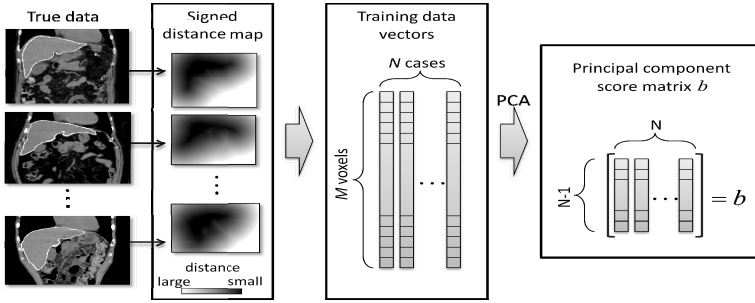


**Fig. 1.** Level set based statistical shape model training

estimation (MAP) [10], followed by the calculation of the same features that were obtained during the construction of matrix X. This set of features from the test image are combined in a column vector  $x_0$ , and will serve as the condition for the conditional SSM. Using matrices  $b$  and X, and the calculated condition  $x_0$ , the conditional average  $\mu_{b|x_0}$  and the conditional covariance matrix  $\Sigma_{bb|x_0}$  are defined as:

$$\mu_{b|x_0} = \mu_b + \Sigma_{bx} \Sigma_{xx}^{-1} (x_0 - \mu_x) \tag{1}$$

$$\Sigma_{bb|x_0} = \Sigma_{bb} - \Sigma_{bx} \Sigma_{xx}^{-1} \Sigma_{xb} \tag{2}$$

with  $\mu_b$  signifying the regular shape model average, derived from matrix  $b$  and  $\mu_x$  denoting the average set of conditional features, derived from matrix X.  $\Sigma_{xx}$  and  $\Sigma_{bb}$  are the covariance matrix of X and  $b$  respectively and  $\Sigma_{xb}$  and  $\Sigma_{bx}$  are mutual covariance matrices. Subsequently, the eigenvectors of the conditional covariance matrix  $\Sigma_{bb|x_0}$  are rearranged in descending order of eigenvalues, after which the top  $L$  modes of variation are selected to form the conditional SSM space, as shown in Fig. 2.

### 3 Relaxed Conditional Statistical Shape Model

A drawback of the conventional conditional SSM is that the selected condition is considered to be reliable. Consequently, if the condition is inaccurate, the conditional SSM will be wrongly influenced and the reconstructed shape will be suboptimal.

To overcome this, a conditional SSM with a relaxed condition is proposed, which is constructed by using a selection formula [5]. To calculate conditional probability, equations (1) and (2) require the set of covariance matrices:

$$\begin{pmatrix} \Sigma_{xx} & \Sigma_{xb} \\ \Sigma_{bx} & \Sigma_{bb} \end{pmatrix}. \tag{3}$$

Following the selection formula, using only a limited range of the conditional features  $x$  results in a new covariance matrix  $V_{xx}$ , and equation (3) can be rewritten as:

$$\begin{pmatrix} V_{xx} & \Sigma_{xb} \\ \Sigma_{bx} \Sigma_{xx}^{-1} V_{xx} & \Sigma_{bb} - \Sigma_{bx} \left( \Sigma_{xx}^{-1} - \Sigma_{xx}^{-1} V_{xx} \Sigma_{xx}^{-1} \right) \Sigma_{xb} \end{pmatrix}. \tag{4}$$

The bottom right term in equation (4) signifies the conditional covariance matrix of  $b$ . Hence, given a conditional range around  $x_0$ , resulting in a covariance matrix  $V_{xx}$ , the covariance matrix for  $b$  can be calculated by:

$$\Sigma_{bb|x_0} = \Sigma_{bb} - \Sigma_{bx} \left( \Sigma_{xx}^{-1} - \Sigma_{xx}^{-1} V_{xx} \Sigma_{xx}^{-1} \right) \Sigma_{xb}. \quad (5)$$

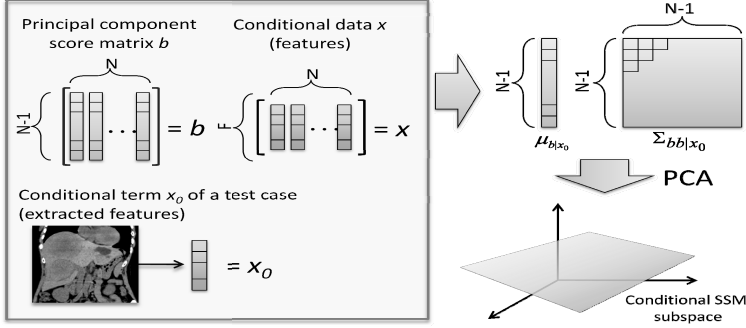


Fig. 2. Construction of the conditional statistical shape model

Note that if the full range of conditional features  $x$  is used, i.e.  $V_{xx} = \Sigma_{xx}$ ,  $\Sigma_{bb|x_0}$  equals  $\Sigma_{bb}$ , corresponding to a non-conditional SSM. In the other extremity, if the range of features  $x$  is limited, such that  $x = x_0$ ,  $V_{xx}$  will become 0 and as a result equation (5) is identical to equation (2), representing the conventional conditional SSM. The average value for  $b$ , given the conditional range around  $x_0$  becomes:

$$\mu_{b|x_0} = \mu_b + \Sigma_{bx} \left( \Sigma_{xx}^{-1} - \Sigma_{xx}^{-1} V_{xx} \Sigma_{xx}^{-1} \right) (x_0 - \mu_x). \quad (6)$$

Analyzing the extremities, similar behavior can be identified, as was observed for the covariance matrix of  $b$ . If the full range of conditional features  $x$  is used, i.e.  $V_{xx} = \Sigma_{xx}$ ,  $\mu_{b|x_0}$  equals  $\mu_b$  (a statistical model without any conditions) and if the range of conditional features  $x$  is limited, such that  $x = x_0$ ,  $V_{xx}$  becomes 0 and equation (6) will be identical to equation (1), representing the conventional conditional SSM.

The difference between the conventional and the relaxed conditional SSM is explained in Fig. 3. As visualized in Fig. 3a, the condition set in the conventional SSM results in a subspace that only comprises the area for which holds  $x = x_0$ . Contrary, for the relaxed conditional SSM, as shown in Fig. 3b, if a selection of samples for which holds that  $x$  approximates  $x_0$  is taken, the fixed condition  $x_0$  is replaced by a relaxed conditional range around  $x_0$ , defined by covariance matrix  $V_{xx}$ .

The relaxed conditional SSM spans from a non-conditional SSM to a conventional conditional SSM. If a small range around  $x_0$  is used to estimate parameter  $b$  (assuming a reliable condition), the model behaves like a conventional conditional SSM. If a large range around  $x_0$  is used to estimate parameter  $b$  (assuming an unreliable condition), the model behaves like a non-conditional SSM. To bridge both SSMs, reliability parameters  $\{\gamma_1, \gamma_2, \dots, \gamma_F\}$  ( $0 \leq \gamma_i \leq 1$ ) are introduced. Since for every conditional feature the error might differ, the reliability parameter  $\gamma_i$  should be defined

individually. In order to reflect the covariance of conditions in the relaxation process, we multiply  $\Sigma_{xx}$  by the reliability parameters, simplifying  $V_{xx}$  to:

$$V_{xx} = \left( (I - \Gamma)^{\frac{1}{2}} \right)^T \Sigma_{xx} (I - \Gamma)^{\frac{1}{2}} \quad (7)$$

with

$$\Gamma = \begin{pmatrix} \gamma_1 & 0 & \cdots & 0 \\ 0 & \gamma_2 & \cdots & 0 \\ \vdots & \vdots & \ddots & \vdots \\ 0 & 0 & 0 & \gamma_F \end{pmatrix} \quad (8)$$

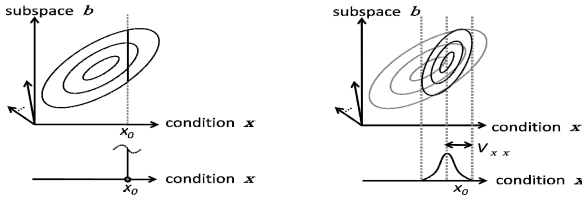


**Fig. 3.** Difference between conventional (left) and relaxed (right) conditional SSM

Substitution of equation (7) into (5) and (6) results in the final equations for the conditional covariance matrix and conditional the average in equations (9) and (10).

$$\Sigma_{bb|x_0} = \Sigma_{bb} - \Sigma_{bx} \left( \Sigma_{xx}^{-1} - \Sigma_{xx}^{-1} \left( \left( (I - \Gamma)^{\frac{1}{2}} \right)^T \Sigma_{xx} (I - \Gamma)^{\frac{1}{2}} \right) \Sigma_{xx}^{-1} \right) \Sigma_{xb}, \quad (9)$$

$$\mu_{b|x_0} = \mu_b + \Sigma_{bx} \left( \Sigma_{xx}^{-1} - \Sigma_{xx}^{-1} \left( \left( (I - \Gamma)^{\frac{1}{2}} \right)^T \Sigma_{xx} (I - \Gamma)^{\frac{1}{2}} \right) \Sigma_{xx}^{-1} \right) (x_0 - \mu_x). \quad (10)$$

This differs from calculating the conditional covariance matrix and the conditional average through ridge regression, which is defined by:

$$\mu_{b|x_0} = \mu_b + \Sigma_{bx} (\Sigma_{xx} + \rho I)^{-1} (x_0 - \mu_x), \quad (11)$$

$$\Sigma_{bb|x_0} = \Sigma_{bb} - \Sigma_{bx} (\Sigma_{xx} + \rho I)^{-1} \Sigma_{xb}, \quad (12)$$

in which  $\rho$  denotes the ridge parameter. In the proposed method the conditional covariance matrix and the conditional average are constructed by multiplication of the original covariance matrix with a value between zero and one, as expressed by equations (9) and (10). Ridge regression adds  $\rho I$  to the original covariance matrix to calculate the conditional covariance matrix and conditional average. The benefit of the proposed method in deriving the conditional covariance matrix and conditional average is that the modifications are proportional to the variance of individual shape variations. Contrary, by adding a fixed ridge parameter, the weaker shape variations are

relatively strongly affected, whereas the influence on the stronger shape variations is limited.

It is worth mentioning that  $\Sigma_{xx}$  might be singular due to multi-colinearity of the features. In experiments, the number of samples was, compared to the number of conditional features, large enough to obtain non-singularity. In addition, from a large data base of features it is easy to select a set of features whose covariance matrix is not singular and which can still be effectively used as conditions for the SSM.

## 4 Estimation of a Shape Prior

The importance of a reliable conditional term in estimating the shape prior was stressed in section 1. To generate the shape prior, the following steps were performed:

1. Roughly extract the test image by maximum a posteriori estimation [10].
2. Project the MAP result onto the relaxed conditional SSM (described in Section 3) and define the parametric position as the search starting point.
3. Select the shape parameters 1 until  $\lfloor L/3 \rfloor$ , in which  $L$  denotes the number of shape parameters that represent 90% of the model's variation.
4. Using Powell's method [11], with the Jaccard Index as objective function, optimize the shape parameters for the projected MAP result.

To avoid local minima, the optimization is done in three subsequent steps: first for shape parameters 1 until  $\lfloor L/3 \rfloor$ , then for 1 until  $\lfloor 2L/3 \rfloor$  and finally for 1 until  $L$ .

## 5 Experimental Setup and Results

The total data set consisted of 144 non-contrast abdominal CT images. The image size was  $512 \times 512 \times 154 \sim 807$  voxels with a resolution of  $0.546 \sim 1.00$  mm/voxel. The data was subsampled by a factor 2. The first 48 cases were used to train the SSM, the second 48 cases were used to decide and evaluate the Graph Cut parameters, to optimize the reliability parameter  $\gamma$  and to optimize  $\rho$ . The third 48 cases, that were available for testing, were divided into two categories: easy to segment and difficult to segment. The state of the art methods in liver segmentation all show acceptable segmentation results for easy cases. For difficult cases however improvements in segmentation can be achieved. This paper therefore will mainly focus on the set of 24 difficult cases. The 24 easy cases will only be discussed briefly. To distinguish between easy and difficult cases, the shape estimates for the 48 test cases were created using a standard, non-conditional SSM. The 24 cases that showed the lowest Jaccard Index after subsequent Graph Cut segmentation were marked as difficult cases.

A set of 20 features, derived from manual labels (training) or from MAP results (testing), was used as conditional terms. Among the features were the object length in  $x$ ,  $y$  and  $z$  direction, surface areas of the projected object on sagittal, coronal and axial planes, the object's volume and histogram derived parameters such as the median  $x$ ,  $y$ , and  $z$  location and the location of the 25<sup>th</sup> and 75<sup>th</sup> percentile  $x$ ,  $y$ , and  $z$  position. Comparing the parameters generated from manual labels with parameters generated

from the MAP results, an average relative error of 4.98% was observed. Because the error rates for the individual features did not differ much, all experiments have been performed with a fixed reliability parameter for all conditions:  $\gamma_1 = \gamma_2 = \dots = \gamma_F = \gamma$ .

Following equations (7) to (10), using different values for  $\gamma$  results in different conditional SSMs.  $\gamma = 0.0$  represents a SSM without conditions,  $\gamma = 1.0$  represents the conventional conditional SSM and the relaxed conditional SSM is constructed in the domain  $0.0 < \gamma < 1.0$ . Within this range the optimal value of  $\gamma$  is searched with intervals of 0.1.  $\gamma = 0.5$  showed best performance in generalization [12] for the relaxed SSM, when using the second 48 cases.

The results obtained by the proposed method were compared with the results obtained through ridge regression (see equations (11) and (12)). The ridge parameter  $\rho$  was optimized by searching for the maximum generalization within a range of  $0.01 \leq \rho \leq 10000$ , in which  $\rho$  was iteratively multiplied by a factor 10. The optimal ridge parameter was found for  $\rho = 1000$ , when using the second 48 cases.

Fig. 4a shows the degree of overlap between the estimated prior and the correct shape, for the 24 selected test cases. Compared to  $\gamma = 0.0$  and  $\gamma = 1.0$ , a reliability parameter of  $\gamma = 0.5$  generates the best results. The shape prior estimation for  $\gamma = 0.5$

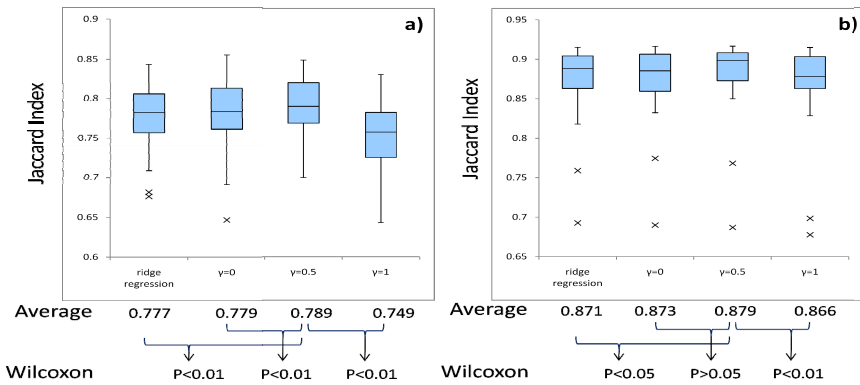


**Fig. 4.** Degree of overlap between shape prior and true shape (a) and between liver segmentation results and the true shape (b) for (from left to right) ridge regression and the proposed method with  $\gamma = 0.0$ ,  $\gamma = 0.5$  and  $\gamma = 1.0$ . Results for 24 difficult cases.

also outperforms shape prior estimation using ridge regression. Despite the small differences, the Wilcoxon signed rank test showed statistical significant differences. Fig. 5 shows an example result of a constructed shape prior. The relaxed conditional SSM ( $\gamma = 0.5$ ) outperforms the other models. Notoriously difficult to segment areas, such as at the tip of the left lobe and at the bottom of the right lobe of the liver show better shape estimation results for the relaxed conditional SSM.

The Graph Cut based liver segmentation used the following energy function:

$$E(A) = \sum_{p \in P} \lambda \cdot R_p(A_p) + \sum_{(p,q) \in NB} \{B_{pq}(A_p, A_q) + S_{p,q}(A_p, A_q)\} \cdot \delta_{A_p \neq A_q}, \quad (13)$$

$$\delta_{A_p \neq A_q} = \begin{cases} 1 & (\text{if } A_p \neq A_q) \\ 0 & (\text{if } A_p = A_q) \end{cases}, \quad (14)$$

in which  $P$  is the set of voxels in CT images,  $p \in P$  denotes the voxels,  $NB$  denotes the set of neighboring voxel pairs,  $A = (A_1, \dots, A_p, \dots, A_{|P|})$  is the set of labels assigned to all voxels and  $\lambda$  is the weight factor to balance both energies. The other parameters are:

$$R_p(A_p) = \begin{cases} -\Pr(I_p | "obj") \Pr("obj") & (\text{if } A_p = "obj") \\ -\Pr(I_p | "bkg") \Pr("bkg") & (\text{if } A_p = "bkg") \end{cases}, \quad (15)$$

$$B_{pq}(A_p, A_q) = \exp\left(-\frac{(I_p - I_q)^2}{2\sigma^2}\right) \frac{1}{\|p - q\|}, \quad (16)$$

$$S_{p,q}(A_p, A_q) = \sqrt{\frac{1}{2} \left( 1 - \frac{\overline{pq} \cdot \nabla \Phi_p}{\|pq\| \|\nabla \Phi_p\|} \right)} \quad (17)$$

with  $I_p$  signifying the CT value of voxel  $p$ . Equation (15) calculates for every voxel the negative likelihood, equation (16) is the boundary term and equation (17) is the shape energy term. In this equation,  $\Phi$  is the signed distance to the outline of the shape prior. By calculating the inner product of the vector from voxel  $p$  to neighboring voxel  $q$  with  $\nabla \Phi_p$ , the validity of the segmented shape is evaluated. Using the second set of 48 cases, optimized values were found at  $\lambda = 1.5$  and  $\sigma = 10.0$  (for ridge regression, for  $\gamma = 0.0$  and for  $\gamma = 1.0$ ),  $\lambda = 1.0$  and  $\sigma = 5.0$  (for  $\gamma = 0.5$ ).

Fig. 4b shows the degree of overlap between the true shape and the result of Graph Cut segmentation with shape priors obtained from ridge regression and obtained from the proposed method with  $\gamma = 0.0$ ,  $\gamma = 0.5$  and  $\gamma = 1.0$ , when using the 24 difficult

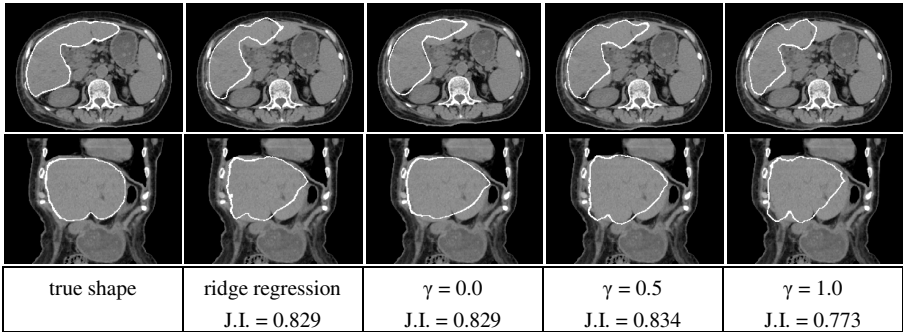


**Fig. 5.** Axial (top row) and coronal (bottom row) example results of generated shape priors for ridge regression and for the proposed method with different values of  $\gamma$

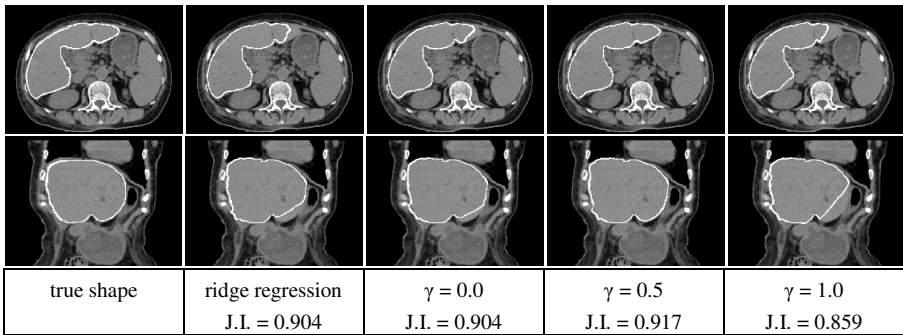


**Fig. 6.** Axial (top row) and coronal (bottom row) example segmentation results for Graph Cuts initialized with different shape priors

cases from the test data set. Wilcoxon signed rank test showed no statistical significant difference between the results for the standard SSM and the relaxed conditional SSM segmentation results. However, comparing the results obtained with the conventional and the relaxed SSM showed a statistical significant difference. Also, the proposed method ( $\gamma = 0.5$ ) outperforms Graph Cut segmentation in which the shape prior was estimated using ridge regression, with a statistically significant difference in performance. Fig. 6 shows an example segmentation result for the four different models and, similar to Fig. 5, the relaxed conditional SSM generates the best results. The example image shows a liver with an extremely large left lobe. The axial view in Fig. 5 clearly shows the performance gain by the strongly improved segmentation of the tip of the left liver lobe. The coronal view shows that, contrary to the other models, the proposed relaxed conditional SSM is able to properly segment the bottom of left lobe, despite its far from average shape.

The 24 easy cases showed comparable results as the difficult cases, with differences however having weaker statistical significance. Average Jaccard Index values for ridge regression,  $\gamma = 0.0$ ,  $\gamma = 0.5$  and  $\gamma = 1.0$  were 0.821, 0.820, 0.826 and 0.800 for shape estimation and 0.922, 0.929, 0.928 and 0.925 for subsequent Graph Cut segmentation. Average evaluation time for MAP based rough segmentation (Intel® Xeon® E5606 CPU), shape estimation (Nvidia® Tesla C2050 GPU) and Graph Cut segmentation (Intel® Xeon® E5606 CPU) were 20, 130 and 20 seconds respectively.

## 6 Discussion

This paper described the construction of a shape prior by a novel relaxed conditional SSM. The generated shapes were used as shape priors for Graph Cut segmentation of the liver in abdominal CT images. This way, the reliability of the condition is taken into account during the generation of the shape prior. A fixed reliability parameter  $\gamma$  was used for all conditions and was optimized using a data set of 48 training cases. Future work will focus on using different values of  $\gamma$  for individual features.

The goal of the research presented in this paper was to improve the accuracy of estimated shape priors. Compared to a conventional conditional SSM, compared to a SSM without condition and compared to a conditional SSM based on ridge

regression, the generated shape priors showed statistical significantly higher accuracy, for the 24 selected difficult to segment cases, thereby achieving the goal of this paper.

Because ridge regression is the only comparable method to bridge between the non-conditional SSM and the conventional conditional SSM, both using a conditional covariance matrix and a conditional average, the results of the proposed method have been compared with ridge regression based shape prior estimates. The proposed relaxed conditional SSM proved to estimate statistical significantly better shape priors.

Evaluating Fig. 4, the benefit of the proposed relaxed conditional SSM clearly lies in improved shape estimation and improved segmentation for difficult to segment images. Inspection of notoriously difficult to segment areas, such as shown in Figs. 5 and 6, corroborate the suggested benefit of the proposed method.

After Graph Cut segmentation, the results based on the relaxed conditional SSM still showed the highest Jaccard Index, also when compared with ridge regression based results. The proposed relaxed conditional SSM showed a higher average segmentation accuracy than all other models, with differences being statistically significant, except when compared to the non-conditional SSM. The improved accuracy in comparison with segmentation based on the conventional conditional SSM was found statistically significant. Therefore, it can be concluded that the relaxed conditional SSM outperforms the conventional conditional SSM, both in the estimation of the shape prior and in the subsequent segmentation.

The calculation of the conditional covariance matrix and the conditional average allows a seamless transition between the generic non-conditional SSM and the conventional conditional SSM. Contrary to [6], in which only a conditional covariance matrix is used, the proposed method calculates both a conditional covariance matrix and a conditional average. Following equations (7) to (10) a perfect interpolation between the non-conditional SSM and the conventional conditional SSM is achieved.

In ridge regression there is an over-accentuation of the weaker shape variations, which are more strongly influenced by the ridge parameter than the stronger shape variations. Such an imbalance does not arise when calculating the conditional covariance matrix and conditional average through equations (9) and (10). The improved performance in shape estimation and its influence on subsequent Graph Cut segmentation can be contributed to this seamless transition between the non-conditional SSM and the conventional conditional SSM.

Future work includes modifications to the algorithm, to enable the processing of contrast enhanced CT data as well. This will also allow a more thorough comparison with other methods, for example based on the SLIVER07 database [13].

**Acknowledgements.** Part of this research was performed under a Grant-in-aid for scientific research from the Japanese Ministry of Education, Culture, Sports, Science and Technology.

## References

1. Boykov, Y., Funka-Lea, G.: Graph Cuts and Efficient N-D Image Segmentation. *Int. J. Comput. Vis.* 70, 109–131 (2006)
2. Freedman, D., Zhang, T.: Interactive Graph Cut Based Segmentation with Shape Priors. In: *IEEE Computer Vision and Pattern Recognition*, pp. 755–762. IEEE Press, New York (2005)

3. Shimizu, A., Nakagomi, K., Narihira, T., Kobatake, H., Nawano, S., Shinozaki, K., Ishizu, K., Togashi, K.: Automated Segmentation of 3D CT Images Based on Statistical Atlas and Graph Cuts. In: Menze, B., Langs, G., Tu, Z., Criminisi, A. (eds.) MICCAI 2010. LNCS, vol. 6533, pp. 214–223. Springer, Heidelberg (2011)
4. de Bruijne, M., Lund, M.T., Tanko, L.B., Pettersen, P.C., Nielsen, M.: Quantitative Vertebral Morphometry Using Neighbor-Conditional Shape Models. *Med. Image Anal.* 11, 503–512 (2007)
5. Lord, F.M., Novick, M.R.: *Statistical Theories of Mental Test Scores*, pp. 146–147. Addison-Wesley Publishing Company Inc. (1968)
6. Baka, N., de Bruijne, M., Reiber, J.H.C., Niessen, W., Lelieveldt, B.P.F.: Confidence of Model Based Shape Reconstruction from Sparse Data. In: 7th IEEE International Symposium on Biomedical Imaging, pp. 1077–1080. IEEE Press, New York (2010)
7. Syrkina, E., Blanc, R., Szekely, G.: Propagating Uncertainties in Statistical Model Based Shape Prediction. In: Proc. of SPIE Medical Imaging, vol. 7962, p. 796240 (2011)
8. Hoerl, A., Kennard, R.: Ridge Regression: Biased Estimation for Nonorthogonal Problems. *Technometrics* 12, 55–67 (1970)
9. Leventon, M.E., Grimson, W.E.L., Faugeras, O.: Statistical shape influence in geodesic active contours. In: IEEE Computer Vision and Pattern Recognition, pp. 316–323 (2000)
10. Shimizu, A., Ohno, R., Ikegami, T., Kobatake, H., Nawano, S., Smutek, D.: Segmentation of Multiple Organs in Non-Contrast 3D Abdominal CT Images. *Int. J. Comput. Assist. Radiol. Surg.* 2, 135–142 (2007)
11. Press, W.H., Teukolsky, S.A., Vetterling, W.T., Flannery, B.P.: *Numerical Recipes*, pp. 509–514. Cambridge University Press (2007)
12. Styner, M.A., Rajamani, K.T., Nolte, L.-P., Zsemlye, G., Székely, G., Taylor, C.J., Davies, R.H.: Evaluation of 3D Correspondence Methods for Model Building. In: Taylor, C.J., Noble, J.A. (eds.) IPMI 2003. LNCS, vol. 2732, pp. 63–75. Springer, Heidelberg (2003)
13. Online Available at: <http://www.silver08.org>